Improved trial eigenfunction in Kinezero

Clarisse Bourdelle
28/07/05

Kinezero solves the gyrokinetic equation using a trial eigenfunction to calculate the eigenvalues. In GS2 or GYRO, both the eigenfunctions and the eigenvalues are calculated from the gyrokinetic equation. It is thanks to its trial eigenfunction that Kinezero can be 380 times faster than GS2 for an identical case.
The choice made for the trial eigenfunction in Kinezero is presented and discussed. It is shown that a simple improvement of the analytical model in the fluid limit allows reproducing well the GYRO and GS2 dependences of the mode width with the magnetic shear s, even at low s. This improved analytical model is implemented and tested in Kinezero.

1. Reminder of the previous choice made in Kinezero

[C. Bourdelle, X. Garbet, G. T. Hoang, J. Ongena, R. V. Budny, Nuclear Fusion **42**, 892 (2002)].

Appendix A.3. Choice for the electrostatic potential

In order to find quickly a growth rate spectrum at each radius, we choose a trial function for the fluctuating electrostatic potential. In our variational approach, $\tilde{\phi}$ is chosen to be the most unstable exact solution obtained in the fluid limit for strongly ballooned modes, so

$$\tilde{\phi}(k_r) = \phi_0 \frac{w^{1/2}}{\pi^{1/4}} e^{-k_r^2 w^2/2} \tag{18}$$

in order to find

$$\int_{-\infty}^{+\infty} \frac{dk_r}{2\pi} |\tilde{\phi}(k_r)|^2 = \int_{-\infty}^{+\infty} dx |\tilde{\phi}(x)|^2 = \phi_0^2.$$

The mode width (w) is calculated in the fluid limit as well, in the case where the interchange is the dominant instability:

$$w^4 = \frac{f_t \frac{q^2}{2\epsilon} \sum_s J_0^2(k_\theta \rho_{cs}) \frac{T_s m_s}{Z_s^2 e^2 B^2}}{f_P \frac{R}{L_s^2} \sum_s J_0^2(k_\theta \rho_{cs}) \frac{T_s e^2 B^2}{m_s} \frac{\sum_s n_s (Z_s^2/T_s)}{\sum_s n_s (T_s/L_{ps})}} \tag{19}$$

with $1/L_{ps} = -\nabla P_s/P_s$, $1/L_s = \nabla q/q$, f_t and f_p being the fractions of trapped and passing particles, respectively.

If $k_\theta \rho_{cs} \gg 1$, the species s becomes adiabatic ($J_0^2(k_\theta \rho_{cs}) \to 0$). The mode width then scales as the species which remains resonant. It should also be noted that when s goes to zero, the mode width diverges to infinity. To avoid this, the mode width is artificially limited to a tenth of the minor radius.

In the fluid limit, the eigenfunction is a gaussian with a width, w, constrained by the balance of the parallel dynamic by the finite Larmor radius effects:

$$f_p \frac{w^2 \dot{k}_{//}^{\,2} c_{eff}^{\,2}}{-\omega^2} = f_t \frac{\delta_{eff}^{\,2}}{w^2} \qquad (1)$$

We assume that the interchange instability is the dominating instability hence $-\omega^2 = \gamma_{\text{int}}^{\,2}$.

We then obtain:

$$w^4 = \frac{f_t \delta_{eff}^{\,2}}{f_p \dot{k}_{//}^{\,2} c_{eff}^{\,2} / \gamma_{\text{int}}^{\,2}} \qquad (2)$$

Equation (2) is identical to equation (19) given in the appendix.

Where f_p and f_t are the fractions of passing and trapped particles, δ_{eff} is an effective banana width, c_{eff} is an effective thermal velocity, $\dot{k}_{//}$ is the radial derivative of the parallel wave vector: $\dot{k}_{//} = \frac{1}{dqR}$ with $d = \frac{1}{n\nabla q}$ the distance between two resonant surfaces in the limit where $d < \frac{1}{\nabla q / q}$.

NB: in the appendix, a factor $\frac{q^2}{\varepsilon^2}$ is missing in the right hand side of equation (19) due to an error in the definition of $\dot{k}_{//}$.

$\dot{k}_{//}$ being proportional to the magnetic shear s, equation (2) leads to: $w \propto \frac{1}{\sqrt{s}}$ and to

$$\frac{d}{w} \propto \frac{1}{\sqrt{s}} \qquad (3)$$

The ballooning representation used in flux tube codes such as Kinezero requires mode widths larger than the distance between two resonant surfaces in order to have a strong overlap between neighbouring modes. The proportionality expressed in (3) shows that for $s \to 0$, $\frac{d}{w} \to \infty$, therefore the ballooning approximation should not be used. We will show in the following that the estimation of the mode width can be sensibly improved in the frame of a simple analytical calculation, calculation in good agreement with GS2 and GYRO calculations solving the eigenfunctions self consistently.

2. Improved analytical mode width model

$w \propto \frac{1}{\sqrt{s}}$ is found assuming modes ballooned at $\theta = 0$. This approximation allowed to simplify the vertical drift dependence in θ and in s, since: $n\omega_{gs} = \frac{-k_\theta T_s}{e_s B} \frac{1}{R}\left(\cos\theta + s\theta \sin\theta\right)$ becomes at $\theta = 0$, $n\omega_{gs} = \frac{-k_\theta T_s}{e_s B} \frac{1}{R}$.

NB: in the ballooning representation, the electrostatic potential is expressed as follows: $\tilde{\phi} = \Phi(\theta) e^{in(\varphi - q(r)\theta)}$, hence the radial wave vector $k_r = \frac{\theta}{d}$, so $\theta = k_r d$.

A more reasonable approximation would be to consider: $\theta \to 0$. In this case:

$$n\omega_{gs} = \frac{-k_\theta T_s}{e_s B}\frac{1}{R}\left(1+\theta^2(s-0.5)\right)$$

The θ dependence modifies the balance from which w is deduced, a part from the parallel dynamic and the finite Larmor radius effect, the interchange term is now playing a role. Nevertheless, a gaussian is still solution of the second order fluid equation.
The gaussian mode width found in this case is:

$$w^4 = \frac{f_t(\delta_{eff}{}^2 + 2d^2(s-0.5))\gamma_{\text{int}}{}^2}{f_p \dot{k}_{//}{}^2 c_{eff}{}^2} \propto \frac{1}{s^2} + \frac{Cte(s-0.5)}{s^4} \qquad (4)$$

Figure 1 illustrates the former $\frac{d}{w}$ dependence versus s of the former model, equation (1), compared to the new formulation, equation (4).

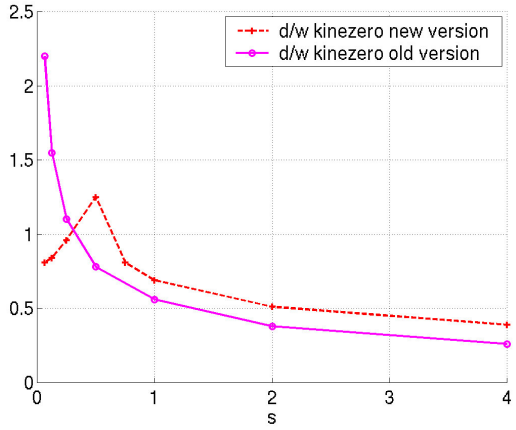

Figure 1: $\frac{d}{w}$ versus s. For $q=2,\ T_e=T_i=4keV,\ n_e=3.10^{19}m^{-3},\ Z_{eff}=1,\ R/a=3$ $r/a=0.5,\ B=3T,\ a\frac{-\nabla T}{T}=8,\ a\frac{-\nabla n}{n}=2,\ k_\theta\rho_s=0.56$.

On Figure 1, with equation (4), $\frac{d}{w}$ does not diverge anymore at $s \to 0$, and for large s, $\frac{d}{w} \to \frac{1}{\sqrt{s}}$ in both cases.

It is of interest to note that for $s=0$ and for any θ, $n\omega_{gs} = \frac{-k_\theta T_s}{e_s B}\frac{1}{R}\cos\theta$, the equation to solve is a Mathieu function and the eigenfunctions are not gaussian but are oscillating Mathieu functions as discussed in appendix B of [J. Candy, R. E. Waltz, and M. N. Rosenbluth, Physics of Plasmas **11**, 1879 (2004)].
In GYRO and GS2, the eigenfunctions illustrate this variety of cases. Shown in figure 2 is an example of an s scan done in both GYRO in its flux tube version and GS2 with the same parameters as for figure 1 for an electrostatic, collisionless, s-α equilibrium case (i.e. same limits as Kinezero)

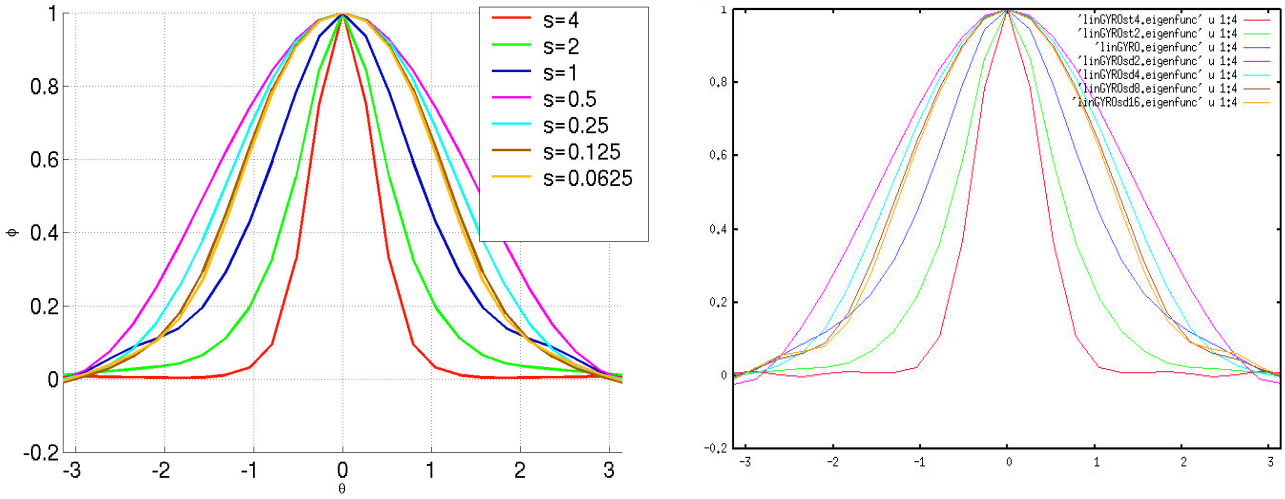

Figure 2: eigenfunctions of GYRO (a) and GS2 (b) normalized to their maximum versus θ between $-\pi$ and π for different values of s.

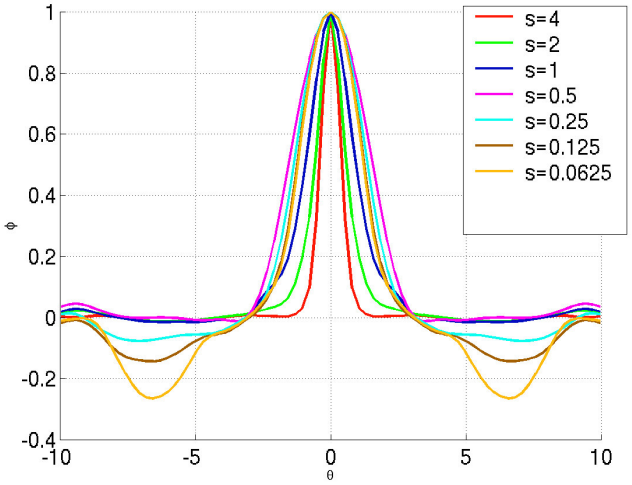

Figure 3: same as 2.a, but wider scale in θ

At $s \leq 0.5$ one can clearly see that the eigenfunctions oscillate for $|\theta| > \pi$, as expected since the solutions tend towards Mathieu functions, whereas at s>0.5 they have a gaussian shape as approximated in Kinezero.

If one assumes that, for $|\theta| < \pi$, the eigenfunctions are gaussian, one can estimate $\frac{d}{w}$ for GYRO and compare with the $\frac{d}{w}$ given by equation (4) using the same parameters as in figure 1.

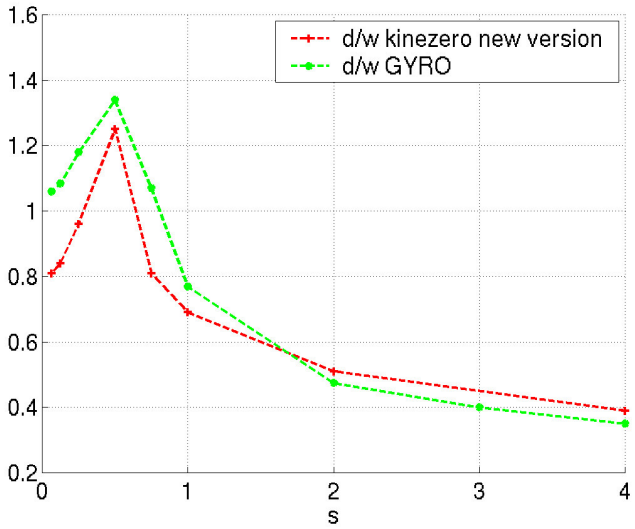

Figure 4: $\frac{d}{w}$ versus s, with w given by equation (4): red crosses, with $\frac{d}{w}$ given by GYRO (figure 2a): green circles.

Around s = 0.5, the sharp variation of $\frac{d}{w}$ for Kinezero is due to the fact that the limit $\theta \to 0$ accentuates the change at s=0.5. For s < 0.5, the stronger disagreement is due to the fact mentioned above: that at $s \to 0$, the eigenfunction is not a gaussian anymore but tends towards a Mathieu function. At s > 1, the $\frac{1}{\sqrt{s}}$ dependence for both cases is very clear. Globally, the qualitative and quantitative agreement between the analytical fluid model used in Kinezero and the exact solution computed in GYRO is quite striking.

The growth rates behaviour with respect to s is modified by the new mode width model only for $s \leq 0.5$ as illustrated on figure 5.

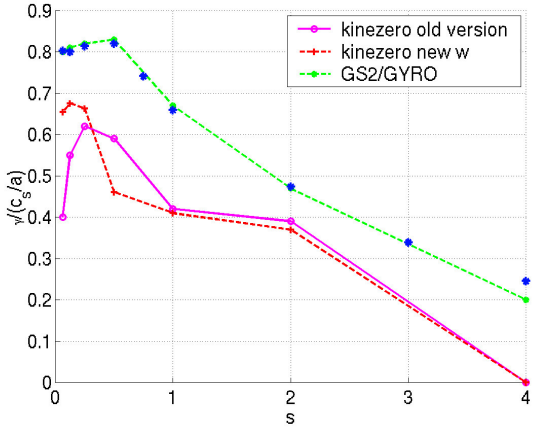

Figure 5: normalized growth rates, $\frac{\gamma}{c_s / a}$, at $k_\theta \rho_s = 0.56$ with the same parameters as figure 1.

Green dashed line: GS2, blue asterisks: GYRO, magenta circles: Kinezero mode width given by equation (2), red crosses: Kinezero mode width given by equation (4)

At low s, the growth rates converge versus a fixed value, as found with both GS2 and GYRO. At $s > 0.5$ The growth rates behaviour remains almost unchanged by the modification of the mode width model as can be seen on figure 6 for the s=1 case. For $s < 0.5$, the growth rates

obtained with equation (4) are closer to GS2 growth rates for both ETG and ITG-TEM as can be seen on figures 6.c and 6.d for s=1/16.

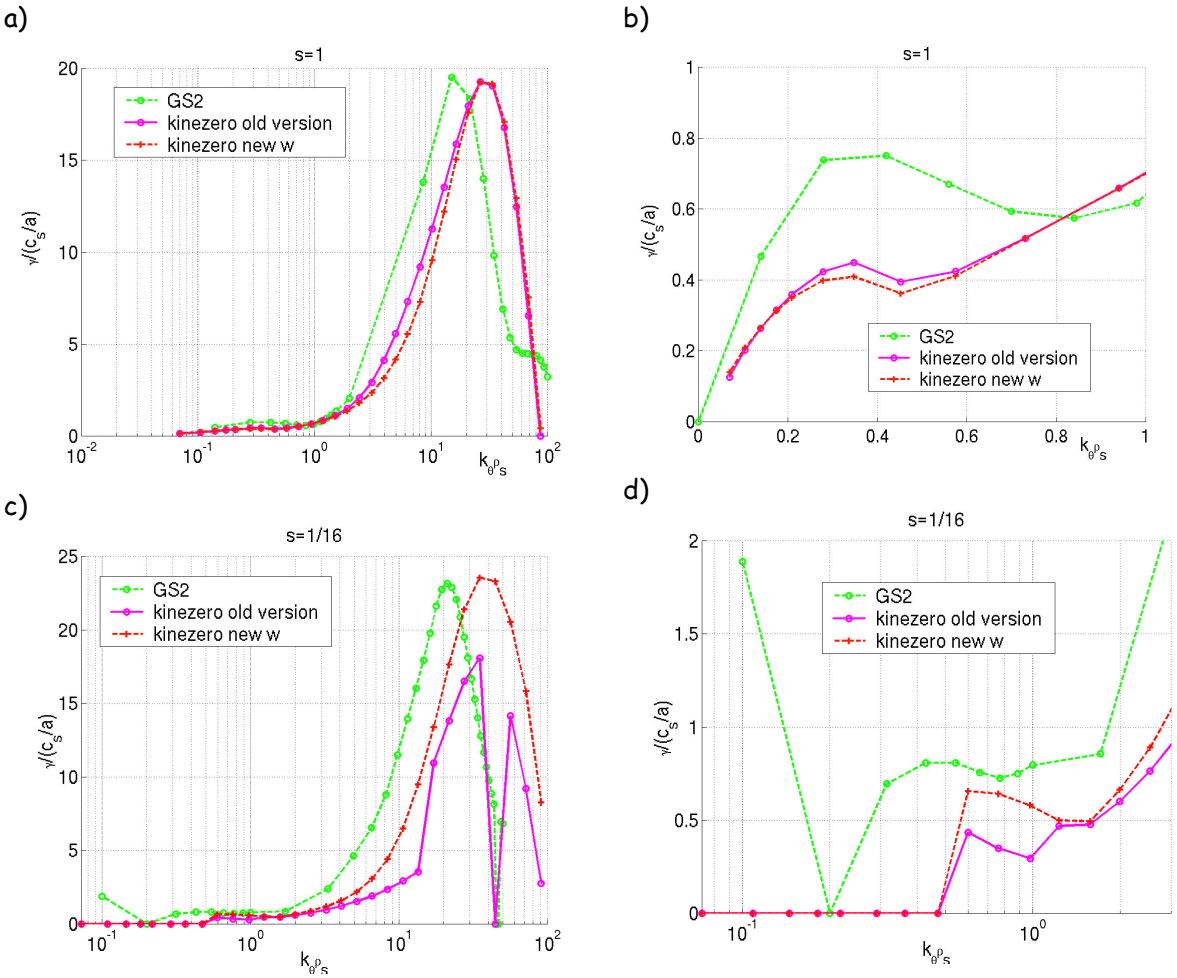

Figure 6: normalized growth rates spectra, $\frac{\gamma}{c_s / a}$ *versus* $k_\theta \rho_s$ *with the same parameters as figure 1 with s= 1 a) and b), at s=1/16 c) and d). Green circles : GS2, magenta circles: Kinezero mode width given by equation (2), red crosses: Kinezero mode width given by equation (4). a) and c)Whole spectra, from ITG to ETG at s=1. b) and d) Zoom on ITG-TEM part.*

Nevertheless, for $k_\theta \rho_s < 1$, the growth rates given by Kinezero are under-evaluated when compared with GS2 as shown on figures 6.b and 6.d, and on figure 5 for all values of s. This under-evaluation is attributed to different ways of accounting for the bounce average and the finite Larmor radius effects in Kinezero and GS2/GYRO as discussed in the note on "finite Larmor radius and finite banana width effects".